

# Superposed 16-QAM Signal Detection Using GaBP in a Massive MIMO System

Taisei Watabe\*, Toshihiko Nishimura\*, Takeo Ohgane\*, Yasutaka Ogawa\*, and Junichiro Hagiwara\*

\* Graduate School of Information Science and Technology, Hokkaido University

E-mail: {watabe, nishim, ohgane, ogawa, jhagiwara}@m-icl.ist.hokudai.ac.jp

**Abstract**—Gaussian belief propagation (GaBP) has been proposed to detect a large number of signals. It is based on message passing of the second-order complexity. In general, the GaBP uses bit-wise reliability. Thus, it is not straightforward to apply the GaBP to the multi-level-modulated signals. In this paper, we propose to compose a 16-QAM symbol from two QPSK symbols using superposition modulation and evaluate the detection performance of the GaBP for superposed 16-QAM signals in a massive MIMO system. In the uncoded case, the uniform and Gray-mapped 16-QAM provides the best performance. However, in the coded case, the performance of superposed 16-QAM becomes much better and outperforms the uniform and Gray-mapped 16-QAM. Thus, the potential capability of superposition modulation in the GaBP detection has been confirmed.

## I. INTRODUCTION

Multiple-input multiple-output (MIMO) transmission is a useful technique to improve the channel capacity almost in proportion to the number of transmit or receive antennas, whichever is smaller [1]. In recent years, massive MIMO systems have been extensively studied to accommodate exponentially-increasing traffic [2], [3]. The massive MIMO means to have 100 or more antenna elements at the base station. At present, the total number of antennas of multiple user terminals is much less than 100. But, in coming the IoT era, massive uplink access will be common.

Detecting the massive signals requires very complex calculations. For example, the complexity of linear spatial filtering is  $O(M^3)$  where  $M$  is the number of transmitted signals. Thus, a signal detection technique called as Gaussian belief propagation (GaBP) has attracted attention recently [4]–[6]. The GaBP expresses the problem as a factor graph and estimates the transmitted signals by iteratively exchanging the reliability information between the variable and factor nodes. The marginalization of conditional probabilities is eliminated by Gaussian approximation for the interference signals. Thus, the complexity of  $O(M^2)$  is achieved.

Applying the GaBP to detecting multi-level-modulated signals is not so simple. A use of bit-wise reliability needs marginalization [7]. So, a use of symbol-wise reliability has been proposed [8]. In this paper, we propose an alternative approach based on superposition modulation [9]. The superposition modulation can decompose a multi-level-modulated signal into primitive elements. For example, a 16-QAM symbol is composed of two QPSK symbols which are suitable to be detected by GaBP. In compensation for such decomposition, however, the number of symbols to be detected is doubled.

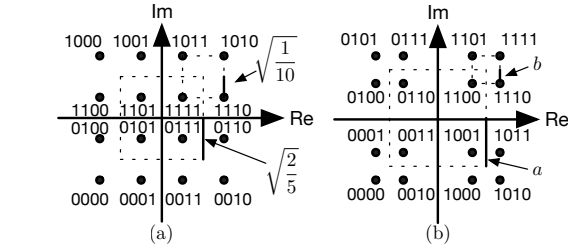


Fig. 1. Examples of 16-QAM constellations. (a) Uniform and Gray mapping, (b) nonuniform mapping using superposition modulation.

Then, overall performance may be degraded. So, we evaluate the detection performance using GaBP for superposed 16-QAM signals in a massive MIMO system and discuss the availability of superposition modulation.

## II. MIMO SYSTEM WITH SUPERPOSED 16-QAM

Consider a MIMO system having  $M$  transmit-antennas and  $N$  receive-antennas. We assume a spatial multiplexing scheme where independent signals are transmitted from each antenna element. Specifically, we also assume that all signals are modulated using 16-QAM.

Fig. 1 shows examples of 16-QAM constellations. The uniform signal constellation as in Fig. 1(a) is commonly used. The minimum Euclidean distance becomes  $\sqrt{2/5}$  at any row and column when the symbol energy is set to one. Gray mapping is generally used so that each adjacent symbol differs in one bit.

As an alternative way to generate 16-QAM symbols, we apply superposition modulation [9]. Then, a 16-QAM symbol is expressed by superposition of two QPSK-signals as in Fig. 1(b). It can be formulated as

$$x_{sp} = \sqrt{2}ax_1 + \sqrt{2}bx_2, \tag{1}$$

where  $x_{sp}$  is a 16-QAM symbol superposition-modulated.  $x_1$  and  $x_2$  are QPSK symbols having a constellation in Fig. 2.  $a$  and  $b$  are the lengths shown in Fig. 1(b). By adjusting the parameters  $a$  and  $b$ , we can generate either uniform or non-uniform constellation. Note that the superposition modulation is incompatible with Gray mapping. Thus, there are some cases where adjacent constellation points differ by two bits.

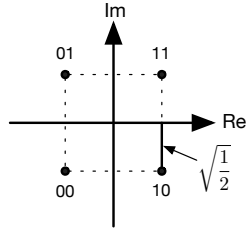


Fig. 2. A QPSK constellation where the symbol energy is set to one.

In order to maintain the symbol energy of  $x_{sp}$  as one under the condition that  $|x_1|^2$  and  $|x_2|^2$  are one, we have

$$2a^2 + 2b^2 = 1. \quad (2)$$

Without loss of generality, we can assume  $a \geq b > 0$ . Then, an inequality  $\sqrt{1/2} > a \geq 1/2 \geq b > 0$  holds<sup>1</sup>. In this paper, we use this superposed 16-QAM symbols for transmit signals. Specifically, a sum of two QPSK symbols  $\sqrt{2}a x_{2j-1} + \sqrt{2}b x_{2j}$  is transmitted from the  $j$ th transmit antenna.

Let  $h_{i,j}$  be the channel between the  $j$ th transmit antenna and  $i$ th receive antenna where  $1 \leq j \leq M$  and  $1 \leq i \leq N$ . Then, the  $i$ th received signal is given by

$$y_i = \sum_{j=1}^M h_{i,j} \left( \sqrt{2}a x_{2j-1} + \sqrt{2}b x_{2j} \right) / \sqrt{M} + z_i, \quad (3)$$

where  $z_i$  is a complex Gaussian noise with zero mean and variance  $\sigma^2$ .  $1/\sqrt{M}$  is the coefficient for setting the total transmit power as one.

By replacing  $\sqrt{2/M} h_{i,j} a = h'_{i,2j-1}$  and  $\sqrt{2/M} h_{i,j} b = h'_{i,2j}$ , we can rewrite (3) as

$$y_i = \sum_{j=1}^{2M} h'_{i,j} x_j + z_i. \quad (4)$$

This is expressed as a vector-matrix form as

$$\mathbf{y} = \mathbf{H}\mathbf{x} + \mathbf{z}, \quad (5)$$

where  $\mathbf{x} = [x_1, \dots, x_{2M}]^T$ ,  $\mathbf{y} = [y_1, \dots, y_N]^T$ ,  $\mathbf{z} = [z_1, \dots, z_N]^T$ , and

$$\mathbf{H} = \sqrt{\frac{2}{M}} \begin{bmatrix} h_{1,1}a & h_{1,1}b & \cdots & h_{1,M}a & h_{1,M}b \\ \vdots & \vdots & \ddots & \vdots & \vdots \\ h_{N,1}a & h_{N,1}b & \cdots & h_{N,M}a & h_{N,M}b \end{bmatrix} \quad (6)$$

$$= \begin{bmatrix} h'_{1,1} & h'_{1,2} & \cdots & h'_{1,2M-1} & h'_{1,2M} \\ \vdots & \vdots & \ddots & \vdots & \vdots \\ h'_{N,1} & h'_{N,2} & \cdots & h'_{N,2M-1} & h'_{N,2M} \end{bmatrix}. \quad (7)$$

<sup>1</sup>When  $a = b = 1/2$ , 7 signal points disappear in the constellation due to degeneration.

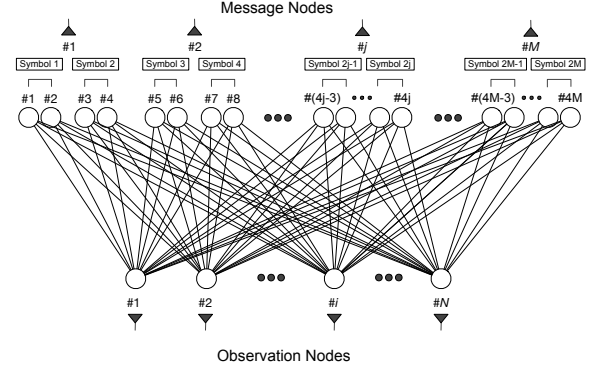


Fig. 3. A factor graph representation for superposed 16-QAM signal detection.

Equations (5) and (7) indicate that a problem detecting  $M$  16-QAM signals is converted into one detecting  $2M$  QPSK signals. Therefore, the detection procedure using GaBP is simplified as will be described below.

### III. DETECTION METHOD BASED ON GABP

#### A. Factor Graph

Fig. 3 shows a factor graph corresponding to (5) and (7) where the variable nodes or message nodes contain the transmitted bit information and the factor nodes or observation nodes contain the received signals. Four bits, i.e., two QPSK signals are mapped per transmit antenna by superposition modulation. Thus, the number of message nodes becomes  $4M$  whereas the number of observation nodes is  $N$ . Note that the strength of the edges connected to the  $j$ th transmit antenna is defined as  $\sqrt{2/M} h_{i,j} a$  or  $\sqrt{2/M} h_{i,j} b$  for  $1 \leq i \leq N$ .

#### B. Processing at Observation Nodes

In the GaBP, soft cancellation is performed at the observation nodes. Log-likelihood ratio (LLR) values passed from the message nodes are used as extrinsic values to generate soft replicas according to the modulation scheme and mapping function. In the paper, we use a QPSK constellation in Fig. 2. Thus, the  $j$ th transmit-symbol replica at the  $i$ th observation node is given by

$$\text{Re}\{\hat{x}_j^{(i)}\} = \frac{1}{\sqrt{2}} \left\{ \tanh \left( \frac{\beta_{2j-1}^{(i)}}{2} \right) \right\} \quad (8)$$

$$\text{Im}\{\hat{x}_j^{(i)}\} = \frac{1}{\sqrt{2}} \left\{ \tanh \left( \frac{\beta_{2j}^{(i)}}{2} \right) \right\}, \quad (9)$$

where  $\beta_{2j-1}^{(i)}$  and  $\beta_{2j}^{(i)}$  are the LLR values passed from the  $j$ th observation node as will be described later. Obviously, the real and imaginary parts of  $\hat{x}_j^{(i)}$  are mutually independent. Note that no LLR values are available at the first iteration. Thus, soft replicas become all zero because the initial values of all extrinsic values are set to zero.

After the replicas are obtained, the soft cancellation is performed at the  $i$ th observation node as

$$\tilde{y}_i^{(j)} = y_i - \sum_{q=1, q \neq j}^{2M} h'_{i,q} \hat{x}_q^{(i)}. \quad (10)$$

Each bit's LLR value is calculated using this signal as [10]

$$\alpha_{2j-1}^{(i)} = 2\sqrt{2} \frac{\text{Re}\{\tilde{y}_i^{(j)} * h'_{i,j}^*\}}{\sigma_e^2} \quad (11)$$

$$\alpha_{2j}^{(i)} = 2\sqrt{2} \frac{\text{Im}\{\tilde{y}_i^{(j)} * h'_{i,j}^*\}}{\sigma_e^2}, \quad (12)$$

where  $\sigma_e^2$  is the equivalent noise power which is a sum of the noise power  $\sigma^2$  and the residual interference power  $\sigma_I^2$  included in  $\tilde{y}_i^{(j)}$ .  $\sigma_I^2$  is obtained by

$$\sigma_I^2 = \sum_{m=1, m \neq j}^{2M} |h'_{i,m}|^2 (1 - |\hat{x}_m^{(i)}|^2). \quad (13)$$

The LLR value  $\alpha_k^{(i)}$  is passed back to the  $k$ th message node.

### C. Processing at Message Node

At the message nodes, first, a posteriori LLR values are calculated using LLR values passed from the observation nodes. Particularly, the a posteriori LLR value at the  $k$ th message node is given by

$$\gamma_k = \sum_{n=1}^N \alpha_k^{(n)}. \quad (14)$$

When channel coding is applied, this a posteriori LLR value is passed to a decoder and is replaced by the decoded output.

The extrinsic value passed to the  $i$ th observation node is obtained by subtracting the LLR value from the  $i$ th observation node to avoid the self information propagation and thus can be expressed as

$$\beta_k^{(i)} = \gamma_k - \alpha_k^{(i)}. \quad (15)$$

### D. Iterative Processing

In the GaBP method, the reliability information expressed as the LLR values is exchanged between the observation and message nodes iteratively and thus the reliability is gradually improved. In this paper, after repeating a predetermined number of updates, the transmitted bits are judged from the a posteriori LLR values at the message node.

### E. Node Selection

It is known that an error-tolerance is different among the bits in any  $m$ -QAM symbol regardless of constellation types, i.e., uniform or non-uniform mapping. For example, in the superposed 16-QAM case,  $x_1$  is error-tolerant than  $x_2$  when  $a > b$  in (1). Thus, the first and the second bits, defined as upper bits, in Fig. 1(b) are expected to have a lower BER compared with the third and fourth bits, defined as lower bits. Node selection is a technique updating the LLR values serially from nodes having higher error resistance [11]. In the case of

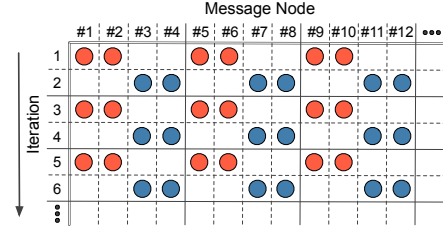


Fig. 4. Staggered update with node selection where error-tolerant nodes are updated first.

TABLE I  
SIMULATION PARAMETERS.

Number of antennas ( $M \times N$ )	100 × 100
Modulation method	Superposed 16-QAM
Channel statistics	Block Rayleigh fading (perfectly known at the receiver)
Noise	White Gaussian noise
Block length	1 symbol duration (200 QPSK symbols)
Number of transmitted blocks	1000 blocks
Maximum iteration number	15 (without node selection) 30 (with node selection)
Channel encoder	(7, 5) convolutional code (constraint length 3, coding rate 1/2)
Channel decoder	Max-log-MAP decoder
Superposition coefficient range	$0 < b < 1/2$

Fig. 1, the error-tolerance has two levels. So, we apply the node selection as shown in Fig. 4 where indices  $i \bmod 4 = 1$  and 2 correspond to the upper bits.

## IV. DETECTION PERFORMANCE

### A. Simulation Environment

Table I shows typical parameters used in the following simulations. We use superposed 16-QAM as described above. The numbers of transmit and receive antenna elements are 100 each. The channel response between each pair of transmit and receive antennas is modeled by uncorrelated block Rayleigh fading, and it is assumed to be known perfectly at the receiver side. 1000 blocks are transmitted for BER evaluation where each block size is one symbol duration, i.e., 200 QPSK symbols.

In coded cases, a (7, 5) convolutional code of constraint length 3 and coding rate 1/2 is used. The maximum iteration number in the GaBP method is set to 15 and 30, with or without node selection, respectively. The superposition coefficients are changed within the range of  $0 < b < 1/2$ . The uniform constellation is achieved by setting  $b = \sqrt{1/10} \approx 0.316$ .

### B. Uncoded Case

Fig. 5 shows the BER performances for the average SNR of 10, 20, and 30 dB in the uncoded case where the superposition coefficient  $b$  is changed from 0 to 0.5. “NS” in the legend

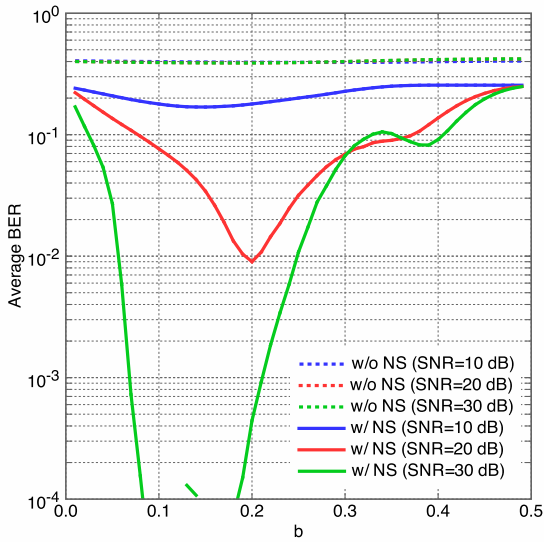


Fig. 5. BER performance versus superposition coefficient  $b$  in uncoded case.

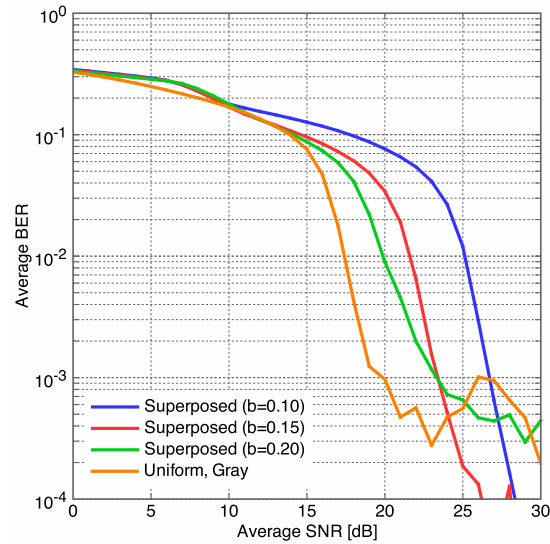


Fig. 6. BER performance versus SNR for superposition coefficient of  $b = 0.10, 0.15,$  and  $0.20$  in uncoded case with node selection.

means “node selection”. All the dotted curves overlap each other. It is clearly indicated that the node selection improves detection performance dramatically. Therefore, in the later evaluation, we use the node selection as an essential technique. Although the optimum  $b$  depends on the SNR, an appropriate range for  $b$  should be from 0.1 to 0.2.

The BER performance versus the SNR is shown in Fig. 6 for  $b = 0.1, 0.15,$  and  $0.2$ , where  $a$  for each  $b$  becomes 0.70, 0.691, and 0.678, respectively. For comparison, we also evaluated the BER performance of uniform and Gray-mapped 16-QAM [7]. The uniform 16-QAM case provides the best performance because of the larger minimum Euclidean distance and Gray-mapping. Although the cliff position for the superposed cases is worse than one for the uniform case, the error floor becomes lower with decrease of  $b$ .

### C. Comparison Between Upper and Lower Bits

Let us check the error tolerance of the upper and lower bits in the superposed cases using the BER performance shown in Fig. 7, where  $b = 0.1, 0.15,$  and  $0.2$ . It is quite reasonable that the BER of the upper bits becomes lower as  $b$  decreases (i.e.,  $a$  increases). Although the BER of the lower bits decreases with increase of  $b$ , an error floor is observed for  $b = 0.2$ . It is supposed that degradation in the detection quality of upper bits strongly affect the detection performance of lower bits.  $b = 0.1$  or  $0.15$  is much less than the corresponding separation in the uniform mapping, and hence the BER cliff becomes worse in such case as in Fig. 6. At present, we conclude that the superposed 16-QAM is not the optimum for uncoded situations. However, it might be possible to improve the detection performance by applying error protection into lower bits.

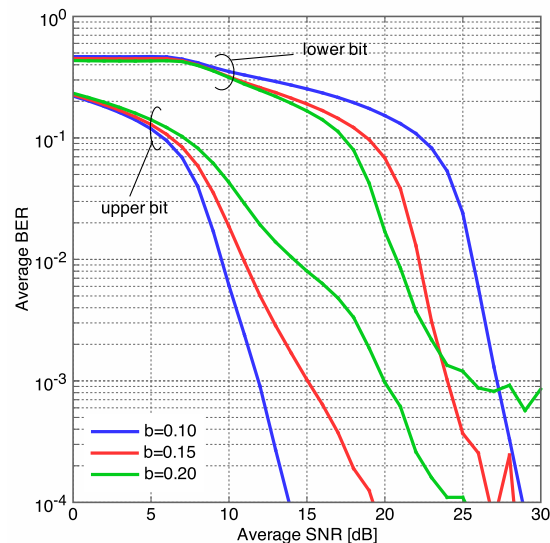


Fig. 7. BER performance of upper and lower bits in uncoded case with node selection.

### D. Coded Case

Finally, we show the BER performance in the coded case as in Fig. 8, where  $b$  is set to 0.08, 0.10, 0.12 which are chosen empirically based on a BER test as in Fig. 5. The coefficient  $a$  for each  $b$  is 0.703, 0.70, and 0.697, respectively. Then, the constellation becomes quite non-uniform. The a posteriori LLR values at the decoder output become much higher than those in the uncoded case. In fact, outliers of the LLR value are observed more frequently in the case of uniform

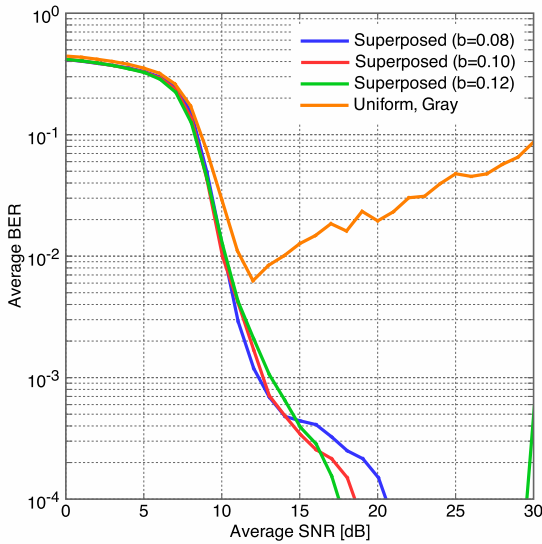


Fig. 8. BER performance for  $b = 0.08, 0.10,$  and  $0.12$  in coded case with node selection.

and Gray mapping, and hence an BER floor can be seen in high SNR region. It is clearly shown that the superposed 16-QAM outperforms the uniform and Gray-mapped 16-QAM for any  $b$  unlike the uncoded case. This performance improvement is definitely given by all of error correction, non-Gray mapping, and unequal error tolerance. It is highly expected that further optimization for these parameters may provide much better performance.

### V. CONCLUSIONS

GaBP based signal detection is an easy and powerful tool for massive MIMO system. However, for higher level modulations, we need additional techniques to obtain a reasonable performance. In this paper, we have proposed using a superposed 16-QAM instead of the uniform and Gray-mapped 16-QAM. Then, the problem detecting  $M$  16-QAM signals is replaced by one detecting  $2M$  QPSK signals. The use of superposed 16-QAM makes the problem structure simpler but scales up to double size. In addition, Gray-mapping cannot be applied. The numerical analysis showed that the detection performance was dramatically degraded when no channel code is used. However, the superposition modulation makes it easy to control the error tolerance of each bit. Thus, applying the node selection which utilizes the difference in error tolerance among the nodes in the factor graph, we could reduce the degradation to about 2.5 dB from the curve for the uniform and Gray-mapped 16-QAM case at the BER of  $10^{-2}$ . Especially, in the coded case, a better performance was obtained by superposition modulation. The parameter setting in this paper is still not optimized yet. Thus, there might be a possibility to improve the detection performance further. More detailed discussion is an urgent issue. On the other hands, the use of

superposition modulation often induces the overloaded MIMO situations. Therefore, another approach which is suitable to overloaded MIMO detection such as [12] instead of GaBP might be a better choice.

### ACKNOWLEDGMENT

This work was supported by JSPS KAKENHI Grant Number JP18H03765.

### REFERENCES

- [1] E. Telatar, "Capacity of multi-antenna Gaussian channels," *European Transactions on Telecommunications*, vol. 10, no. 6, pp. 585–595, Nov./Dec. 1999.
- [2] T. L. Marzetta, "Noncooperative cellular wireless with unlimited numbers of base station antennas," *IEEE Trans. Wireless Commun.*, vol. 9, no. 11, pp. 3590–3600, Nov. 2010.
- [3] F. Rusek, D. Persson, B. K. Lau, E. G. Larsson, T. L. Marzetta, O. Edfors, and F. Tufvesson, "Scaling up MIMO: opportunities and challenges with very large arrays," *IEEE Signal Process. Mag.*, vol. 30, no. 1, pp. 40–60, Jan. 2013.
- [4] P. Som, T. Datta, A. Chockalingam, and B. S. Rajan, "Improved large-MIMO detection based on damped belief propagation," *Proc. ITW 2010*, Jan. 2010.
- [5] T. Wo and P. A. Hoeher, "Low-complexity Gaussian detection for MIMO systems," *Journal of Electrical and Computer Engineering*, vol. 2010, Feb. 2010.
- [6] A. Chockalingam and B. S. Rajan, *Large MIMO systems*, Cambridge University Press, 2014.
- [7] T. Usami, T. Nishimura, T. Ohgane, and Y. Ogawa, "BP-based detection of spatially multiplexed 16-QAM signals in a fully massive MIMO system," *Proc. ICNC 2016 Workshop on CNC*, pp. 166–170, Feb. 2016.
- [8] T. Takahashi, S. Ibi, S. Sampei, "Design of adaptively scaled belief in large MIMO detection for higher-order modulation," *APSIPA ASC 2017*, pp. 12–15, Dec. 2017.
- [9] P. A. Hoeher and T. Wo, "Superposition modulation: myths and facts," *IEEE Commun. Mag.*, vol. 49, no. 12, pp. 110–116, Dec. 2011.
- [10] T. Takahashi, S. Ibi, and S. Sampei, "On normalization of matched filter belief in GaBP for large MIMO detection," *Proc. VTC 2016-Fall*, Sept. 2016.
- [11] M. Hagiwara, T. Nishimura, T. Ohgane, and Y. Ogawa, "Node selection for belief propagation based channel equalization," *IEICE Trans. Commun.*, vol. E100-B, no. 8, pp. 1285–1292, Aug. 2017.
- [12] R. Hayakawa and K. Hayashi, "Error recovery for massive MIMO signal detection via reconstruction of discrete-valued sparse vector," *IEICE Trans. Fundamentals*, vol. E100-A, no. 12, pp. 2671–2679, Dec. 2017.